A Thermally Stable SO₂ Releasing Mechanophore: Facile Activation, Single-Event Spectroscopy, and Molecular Dynamic Simulations

Yunyan Sun^{a,b}, William J. Neary^{a,b†}, Xiao Huang^c, Tatiana B. Kouznetsova^d, Tetsu Ouchi^d, Ilia Kevlishvili^e, Kecheng Wang^a, Yingying Chen^{b,f}, Heather J. Kulik^{c,e*}, Stephen L. Craig^{d*}, Jeffrey S. Moore^{a,b*}

^a Department of Chemistry, University of Illinois at Urbana-Champaign, Urbana, Illinois 61801, United States. ^b Beckman Institute for Advanced Science and Technology, University of Illinois at Urbana-Champaign, Urbana, Illinois 61801, United States. ^c Department of Chemistry, Massachusetts Institute of Technology; Cambridge, Massachusetts, 02139, United States. ^d Department of Chemistry, Duke University, Durham, North Carolina 27708, United States. ^e Department of Chemical Engineering, Massachusetts Institute of Technology; Cambridge, Massachusetts, 02139, United States. ^f Department of Material Science and Engineering, University of Illinois at Urbana-Champaign, Urbana, Illinois 61801, United States

ABSTRACT: Polymers that release small molecules in response to mechanical force are promising candidates as next-generation on-demand delivery systems. Despite advancements in the development of mechanophores for releasing diverse payloads through careful molecular design, the availability of scaffolds capable of discharging biomedically significant cargoes in substantial quantities remains scarce. In this report, we detail a non-scissile mechanophore built from an 8-thiabicyclo[3.2.1]octane 8,8-dioxide (**TBO**) motif that releases one equivalent of sulfur dioxide (SO₂) from each repeat unit. The **TBO** mechanophore exhibits high thermal stability but is activated mechanochemically using solution ultrasonication in either organic solvent or aqueous media with up to 63 % efficiency, equating 206 molecules of SO₂ released per 143.3 kDa chain. We quantified the mechanochemical reactivity of **TBO** by single molecule force spectroscopy and resolved its single-event activation. The force-coupled rate constant for **TBO** opening reaches $\sim 9.0 \text{ s}^{-1}$ at $\sim 1520 \text{ pN}$, and each reaction of a single **TBO** domain releases a stored length of $\sim 0.68 \text{ nm}$. We investigated the mechanism of **TBO** activation using *ab initio* steered molecular dynamic simulations and rationalized the observed stereoselectivity. These comprehensive studies of **TBO** mechanophore provide a mechanically coupled mechanism of multi-SO₂ release from one polymer chain, facilitating the translation of polymer mechanochemistry to potential biomedical applications.

INTRODUCTION

Sulfur dioxide (SO₂), known historically as an environmental pollutant and a food preservative, 1,2 has recently gained recognition as an endogenously generated gaseous signaling molecule (GSM) responsible for transmitting chemical signals in organisms, tissues, and cells.^{3,4} There is mounting evidence that suggests SO₂ may be a fourth gasotransmitter akin to NO, CO, and H2S, but this claim is still being carefully examined and validated.⁵ SO₂ has also been found to be a potent therapeutic agent with various pathophysiological effects, including its abilities in reactive oxygen species (ROS) upregulation and glutathione (GSH) consumption.⁵⁻⁸ Gaseous SO₂ and mixed sulfite salts are traditionally used as the SO₂ donor in biological assessment, leading to concerns in both dosage control and release kinetics. The development of reliable SO₂ donors is therefore highly desirable. ⁶ Whereas a few controllable SO2 donors have been reported under external stimuli such as light, 9-11 heat, 12 chemical reagent, 13-16 and enzymes, 17 the development of SO₂ donors using alternative chemistries and triggering mechanisms will enable new possibilities in future biological investigations. 6,18,19

Polymer mechanochemistry has recently attracted great attention as an enabling tool to release cargo molecules in a controlled manner for potential biomedical applications. ^{20–26} Ultrasound is typically employed as an external trigger to generate solvodynamic shear force from the collapsing

microbubbles.²⁷ The resulting mechanical energy efficiently activates stress sensitive motifs embedded in polymer backbones, known as mechanophores, to release desired payloads. This approach, especially when combined with recent advances in using biomedical ultrasound, ^{28,29} offers promise as a new way to drive chemical reactions remotely, as ultrasound has the unique ability to penetrate deep within biological tissues to achieve mechanochemical transformations noninvasively with precise spatial and temporal control.³⁰⁻³² While the judicious design of mechanophores has enabled the liberation of various molecules upon activation, the scope of cargos that have biomedically relevant functions is still very limited, ^{33–47} especially when high payload is needed.²⁰ The development of non-scissile mechanophores that release many drug-like molecules (e.g., GSMs) per polymer chain is still underexplored.48

Our group recently developed a non-scissile norborn-2-en-7-one (NEO) mechanophore that releases carbon monoxide (CO) upon the application of mechanical stimuli. ⁴⁹ The CO gas was designed to be extruded from an unsaturated [2.2.1] bicyclic ketone motif after the generation of mechano-diradicals from the homolytic activation of C–C bonds (Scheme 1a). We hypothesized that if a sulfone moiety was substituted for the bridging CO in NEO, it would act as an alternative leaving group that would be liberated following a similar pathway, resulting in a new non-scissile SO2 releasing mechanophore.

Scheme 1. (a) Our previous work on NEO mechanophores. (b) Known thermal instability of [2.2.1]-bicyclic sulfones. (c) This work on a thermally stable but mechanically labile SO₂ donor.

Unfortunately, preliminary trials following this strategy were unsuccessful (Scheme S1), presumably due to the welldocumented poor thermal stability of unsaturated [2.2.1] bicyclic sulfones. The spontaneous SO₂ cheletropic extrusion is known to proceed near room temperature when either one or two double bonds are present in the bicyclic ring, generating diene or benzene derivatives respectively (**Scheme 1b**). ^{13,50} To overcome the challenge of thermal decomposition in such scaffolds, we herein report the development and comprehensive investigation of a highly thermally stable but mechanically labile SO₂ releasing mechanophore based on an 8thiabicyclo[3.2.1]octane 8, ,8-dioxide (TBO) scaffold (Scheme 1c). The mechanically triggered release of SO₂ from TBO was demonstrated in both organic solvent (i.e., THF) and aqueous media using pulsed ultrasonication. We quantified the reactivity of TBO under tensile force using single-molecule force spectroscopy (SMFS) and resolved its single-event activation process in force-clamp experiments. The mechanism and stereoselectivity of TBO opening were further investigated using ab initio steered molecular dynamics (AISMD) and results are discussed below.

RESULTS AND DISCUSSION

Synthesis of TBO and Main-Chain TBO Containing Polymers. We set out to synthesize the TBO mechanophore from the cheletropic addition between 1,3-cycloheptadiene and excess liquid SO₂ utilizing a pressure tube (Scheme 2).⁵¹ A clean transformation with excellent yield (93%) was observed after 7 days to afford 1 in multigram scale, whose structure was confirmed by X-ray crystallography. Intriguingly, trials on 1,3cyclooctadiene under the same condition led to no conversion bicyclic an osmium-catalyzed sulfones. Next, dihydroxylation reaction using citric acid as an additive provided 2 in 62% yield. 52 The exo product was observed as the diastereomer, consistent with diastereoselectivity observed in the dihydroxylation of norbornene like structures.⁵³ A subsequent two-step sequence of acylation and ring-closing metathesis afforded macrocycle 4 as an E/Z mixture in 81% yield. The stereochemistry of 4 was confirmed to be the exo product by X-ray crystallography

(Scheme 2). Notably, 19.5 wt% of the monomer 4 comes from SO₂. We copolymerized 4 with Z-cyclooctene using ring-opening metathesis polymerization (ROMP) to obtain multi-mechanophore polymers (MMPs) P1 for solution sonication studies.⁵⁴ Following the common strategy pioneered by the Craig lab, another comonomer 1,2-epoxy-5- cyclooctene was used to prepare 1:1 statistical copolymer P2 for SMFS studies.⁵⁵ The epoxides in the backbone aim to provide strong adhesion to the atomic force microscope (AFM) tip, ensuring the application of nN-regime forces that are typically required to activate covalent bonds.

Scheme 2. The synthesis of TBO embedded polymers for solution sonication and SMFS studies.

Ultrasonic Activation of TBO Mechanophore. The mechanochemical reactivity of **P1** (M_n = 141.1 kDa, D = 1.9, 52.4% TBO, 14.9 wt% from SO₂) was evaluated in dilute THF solutions using pulsed solution ultrasonication (1 s on/1 s off, -10 °C, 20 kHz, 10.0 W cm⁻²). During 120 min of sonication, several new resonance peaks emerged and intensified in ¹H NMR of the resulting material SP1, with a concomitant decrease of all corresponding TBO peaks. The characteristic peak at $\delta = 7.08$ ppm was assigned to the α proton in vinyl ester moieties, suggesting the desired activation of TBO (Figure 1a). The microstructure of SP1 was carefully determined via 2D NMR analysis and was consistent with the formation of a single symmetrical isomer (Figure S3-S8), as evidenced by the one sharp doublet resonance at $\delta = 7.08$ ppm. The $^3J_{\rm HH}$ coupling constant between two new vinyl protons was calculated to be 15.0 Hz (Figure S5), strongly suggesting the trans configuration (i.e., E olefin). The (E,E) isomer was the stereoretentive product from the opening of TBO ring, and the stereoselectivity was similar to our previously reported NEO mechanophores. 49,56 From peak assignments, it was determined

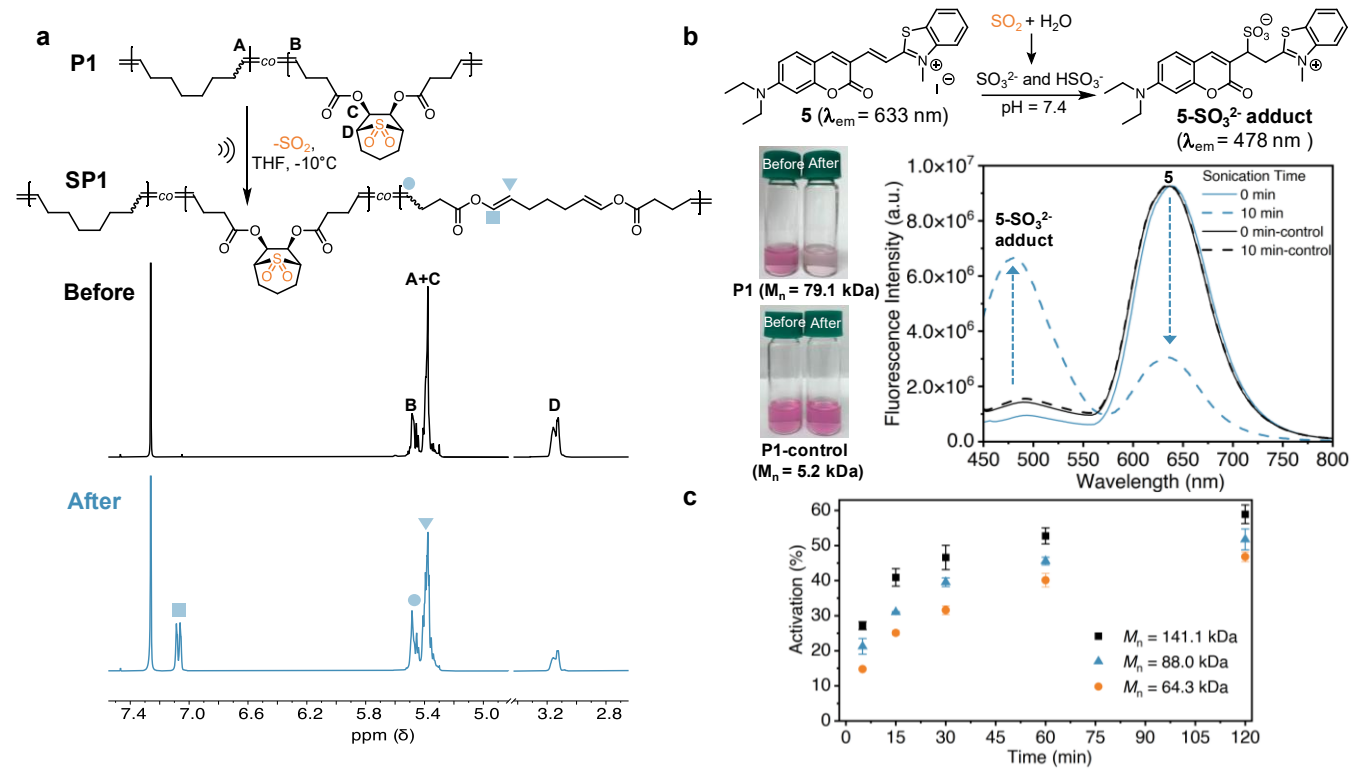


Figure 1. a) Stacked 1 H NMR transformation of P1 (black) to SP1(blue) in CDCl₃ upon sonication. b) The detection of released SO₂ using the fluorogenic probe 5 ($\Phi = 33\%$). The left figures show the color of probe solution with the addition of aliquots before or after sonication. The right figure shows the fluorescent spectra of probe solution with the addition of aliquots at different sonication times. c) Activation 6 (Φ) of P1 with different 6 M_n upon sonication. Φ was determined from the average of three trials.

that 63% of the **TBO** mechanophores were activated after 120 min of sonication based on integrations in ¹H NMR. Low molecular weight P1 ($M_n = 5.2 \text{ kDa}$) was synthesized as control, as it is known that low molecular weight polymers experience negligible elongational force in solution sonication.²⁷ We observed no activation under the same condition in this case, indicating the mechanochemical nature of this transformation (Figure S9). Different from the facile mechanochemical activation, no SO₂ extrusion nor other decomposition of TBO was observed from ¹H-NMR at 120 °C even after 24 h (Figure **S11**). We also conducted thermal gravimetric analysis (TGA) on P1 and did not observe significant weight loss until 300 °C (Figure S12), indicating no thermal SO₂ extrusion upon moderate heating. The saturated design of the [3.2.1] structure effectively shuts down the cheletropic extrusion pathway, accounting for the excellent thermostability.

To confirm the release of SO₂ from P1, we employed a reported fluorogenic probe 5 that selectively reacts with SO₂ derived sulfite (SO₃²⁻) and bisulfite (HSO₃⁻).⁵⁷ Specifically, the nucleophilic attack of SO_3^{2-} and HSO_3^{-} interrupts the π conjugation of a hemicyanine dye, leading to large changes in both absorption and emission spectrums (Figure 1b). After sonication of **P1** ($M_n = 79.1 \text{ kDa}$, $D = 1.8, 48.0 \text{ mol } \% \text{$ **TBO**)for 10 min in THF, an aliquot of the solution was added to a 10 μM PBS buffer solution of 5. The deep purple color of 5 PBS solution disappeared after 20 min of incubation and turned into faded pink color, indicating the generation of 5-SO₃²-adduct. In contrast, negligible color change was observed after incubation without ultrasonication (Figure 1b). The fluorescent spectra were also monitored before and after sonication. We observed the emergence of a new peak at 478 nm with the decrease of the original peak at 633 nm only after sonication, which is

indicative of the generation of 5-SO₃²- adduct (Figure 1b). On the other hand, no significant changes were detected in either the color of the solution or the emission spectrum after the sonication of P1-control ($M_n = 5.2$ kDa). Infrared (IR) spectroscopy analysis was conducted to further elucidate the extrusion of SO₂ in SP1. The significantly diminished intensity of S=O stretching peak at ~ 1305 cm⁻¹ after sonication validated the release of SO₂ (Figure S14).⁵⁸ Additionally, we noticed two new peaks in the IR of **SP1** at 1675 cm⁻¹ and 934 cm⁻¹. These peaks correspond to the stretching and bending of transdisubstituted olefins respectively, in agreement with the proposed vinyl ester groups generated upon activation.⁵⁸ We note that the direct ultrasound triggered SO₂ release was previously observed in the depolymerization of alternating sulfone copolymers.⁵⁹ However, the co-release of many vinyl acetate monomers and the lack of backbone tunability make those polymers impractical as reliable SO2 donors compared to TBO.

Controlling the local concentration is critical for GSMs delivery, as a number of GSMs including SO₂ are known to show critical regulatory functions only at low concentrations, while exhibiting systemic toxicity at high concentrations. ⁶⁰ To demonstrate the tunable release rate of **TBO**, various molecular weight **P1** samples were synthesized, and the kinetics of activation were investigated. The activation percentage (Φ) was monitored by ¹H NMR (**Figure 1c**). We observed a faster **TBO** activation with the increase of molecular weight, in agreement with other reported MMPs. ^{49,61} By tuning the molecular weight and/or the sonication time, **TBO** activation percentage from 14% to 63% were achieved (**Table S1-S3**). For **P1** of 64.3, 88.0, and 143.3 kDa, up to about 73, 115, and 206 SO₂ molecules are

released on average per polymer chain after 120 min of sonication, respectively (See SI for more details).

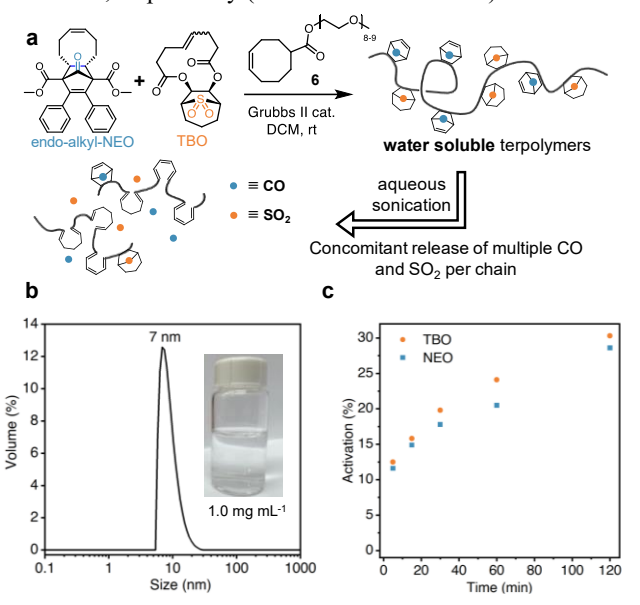


Figure 2. a) The preparation of water soluble terpolymers that release CO and SO₂ concomitantly upon sonication. b) The size of polymers dispersed in water measured by dynamic light scattering and the corresponding photo. c) Activation % (Φ) of two mechanophores in terpolymers upon sonication determined by ¹H-NMR.

Triggering the activation in aqueous conditions is required to translate cargo releasing mechanophores to biomedical applications. However, the mechanochemical activation of the cargo releasing mechanophore systems, especially for MMPs, has been mostly investigated in pure organic solvents or their mixtures with water. 26,35,37,43,44,48 In pursuit of both good solubility in water and reasonable incorporations of TBO in the polymer main chain, we synthesized comonomer 6 that contains a ROMP compatible cyclooctene motif with a grafted short polyethylene glycol (PEG) unit (Figure 2a). The resulting high molecular weight copolymers ($M_n = 597.8 \text{ kDa}$, D = 2.3) with 20.6 mol% of TBO (2.9 wt% from SO₂) readily dissolved in water with moderate aggregation (Figure S18). The application of ultrasound to 1.0 mg mL⁻¹ copolymer solution (1 s on/1 s off, ice bath, 20 kHz, 10.0 W/cm²) provided 67% of TBO activation after 60 min, equating the generation of ~ 300 μM of SO₂ (Figure S19). We also copolymerized monomer 4 and monomer 6 with our previously developed CO-releasing endoto generate statistical terpolymers alkyl-NEO concomitantly release CO and SO2 from one polymer chain as an approach for the co-delivery two GSMs (Figure S20).⁵⁶ The size of the resulting terpolymer ($M_n = 304.6 \text{ kDa}$, D = 2.4, 15.9 mol% NEO, 13.9 mol% TBO) in water was determined to be around 7 nm on average using dynamic light scattering (DLS) (Figure 2b). From the kinetic study of sonication, we observed slightly greater activation rate of TBO compared to endo-alkyl **NEO** (Figure 2c). Reasonable Φ values around 30% were achieved for both mechanophores upon 120 min of sonication, corresponding to around 92 µM of SO₂ and 99 µM of CO. We envision these aqueous soluble copolymers as promising materials for biomedical applications in combination with biocompatible ultrasound in future studies.²⁹

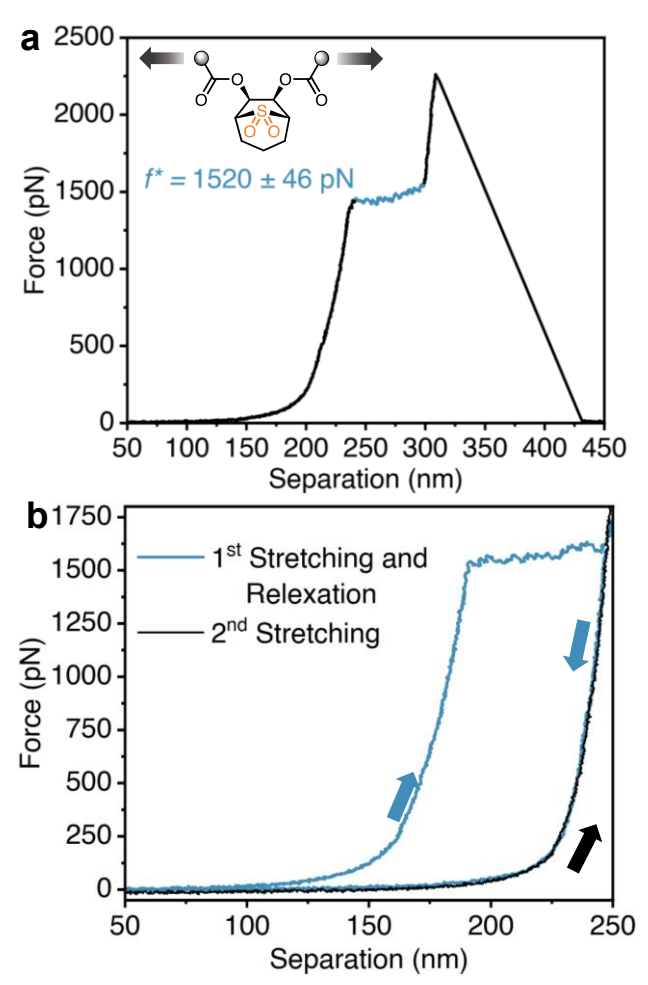


Figure 3. a) Representative force—extension curve of P2 in toluene ($M_n = 73.6$ kDa, D = 1.8, TBO % = 47.2 mol %); retraction velocity = 300 nm s⁻¹. b) Representative retracing force curves of P2.

Single-Molecule Force Spectroscopy of TBO. To quantify the mechanochemical reactivity of TBO and compare it with other reported mechanophores, we used SMFS to directly measure the transition force (f^*) in a kinetic regime relevant to most potential applications.^{62–68} We prepared **P2** with relatively high molecular weights and **TBO** incorporations ($M_n = 73.6$ kDa, D = 1.8, **TBO** mol% = 47.2) to sample a large number of mechanophores along one polymer chain.

Representative force vs separation curves obtained from constant-velocity (CV) SMFS experiments are shown in Figure 3a. In CV SMFS, the tip of the atomic force microscope (AFM) and the substrate on which the polymer is deposited are separated at a constant retraction velocity of 300 nm s⁻¹. As a polymer chain that is attached to both surfaces is stretched, the corresponding force along its backbone gradually increases. Eventually, the force becomes high enough to accelerate the TBO reaction to observable rates. These reactions result in the lengthening of the polymer. Further stretching continues to accelerate the reaction, and as the rate at which the polymer lengthens approaches the rate at which the polymer is being stretched (300 nm s⁻¹), a plateau appears in the force-separation curve. The plateau is characterized by a transition force, f^* , taken from the inflection point of the transition. The absolute rate of chain extension at a given force is proportional to the total number of mechanophores in the trapped region of the

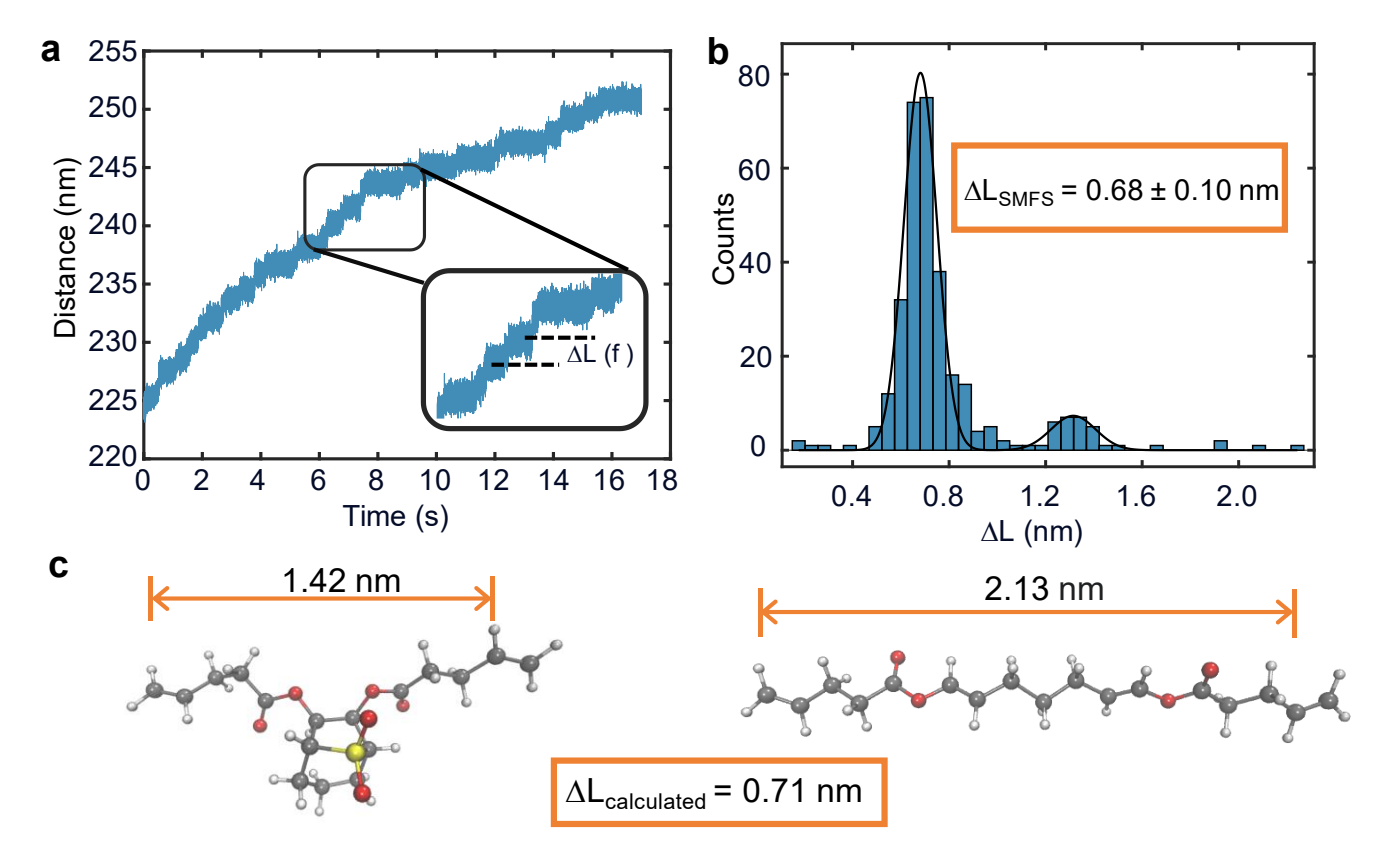


Figure 4. a) Representative distance vs time curves for P2 at 1440 pN, obtained by constant-force SMFS. Insets highlight the staircase pattern and extraction of stored length release per activation. b) Histograms of changes in polymer contour length per detected activation, obtained from constant-force experiments for polymers **P2**. All bin sizes are 0.05 nm, and the histograms were fitted with a Gaussian distribution (black curve). c) Calculated geometries of **TBO** repeating unit and their associated end-to-end distances in both their nascent and fully unraveled states, obtained from EFEI under 1440 pN of force. In the fully unraveled states, the released SO₂ does not contribute to the stored length and it is therefore not included.

polymer, and so f^* in CV SMFS varies with both the length of the trapped chain region and with the loading of mechanophore along the backbone.

In the case of the **TBO** polymers examined, f^* was determined to be 1520 ± 46 pN (**Figure 3a**). The relatively low f^* value of **TBO** indicates its higher reactivity compared to most cyclobutane and ladderane mechanophores, 63,68,69 and it is comparable to the *exo*-alkyl-**NEO** mechanophore reported by us previously ($f^* = 1526 \pm 33$ pN). We also performed retracing experiments and observed full hysteresis (i.e., no plateau in the 2^{nd} stretching) (**Figure 3b**), implying the irreversible activation of **TBO** in SMFS.

To further characterize **TBO** mechanochemistry, we obtained the distance vs time curves of **P2** using the complementary technique of constant-force SMFS, also known as force-clamp (FC) spectroscopy. In FC experiments, feedback control of the AFM allows the polymer chains to be held at a constant tension that is maintained by automated adjustment of the tip position to restore force that is lost when a **TBO** opening releases stored length that relaxes the chain. Here, polymer chains were successfully clamped for up to 18 s at average forces of 1440 pN, just below the plateau force observed in the CV SMFS experiments (**Figure 4a and more details in the SI**). As the high force is applied to **P2** over this time, the **TBO** mechanophore will open, extend, and release the stored length in the seven membered ring, leading to an increase in the polymer contour length. These events lead to jumps in the

distance vs time curves, and the time between events reflects how much time the polymer spends at a given degree of unravelling before another unravelling event occurs.

Using this approach, we were able to resolve the single activation event of TBO mechanophore in the FC experiments at the applied force of 1440 pN, as evidenced by the staircase pattern shown in Figure 4a. 70 The distribution step sizes (ΔL) were characterized across all the pulls and used to determine the average change in length between two steps. Fitting the collected data with a Gaussian distribution yields the average value of 0.68 ± 0.10 nm for **P2** (Figure 4b). To validate the nature of the observed transitions, we calculated the contour length of the TBO repeating unit before and after activation under the experimental force (i.e., 1440 pN), using the external force explicitly included (EFEI) method. 71,72 The optimized equilibrium geometries of the nascent TBO and its fully unraveled state were calculated under 1440 pN as shown in Figure 4c. The simulated stored length of a single TBO unit equals 0.71 nm, in good agreement with the experimental results from SMFS. A second small peak is observed in the experimental distribution of step sizes (Figure 4b). The corresponding ΔL value for that second peak is 1.32 ± 0.13 nm (Figure S35), and that value is consistent with the activation of two TBO mechanophores that cannot be resolved individually. Looking forward, the overall gain in length enabled by TBO makes it a potential candidate for reactive strand extension in the service of tougher bulk polymeric networks.^{73,74} The bifunctional character of the TBO mechanophore (i.e.,

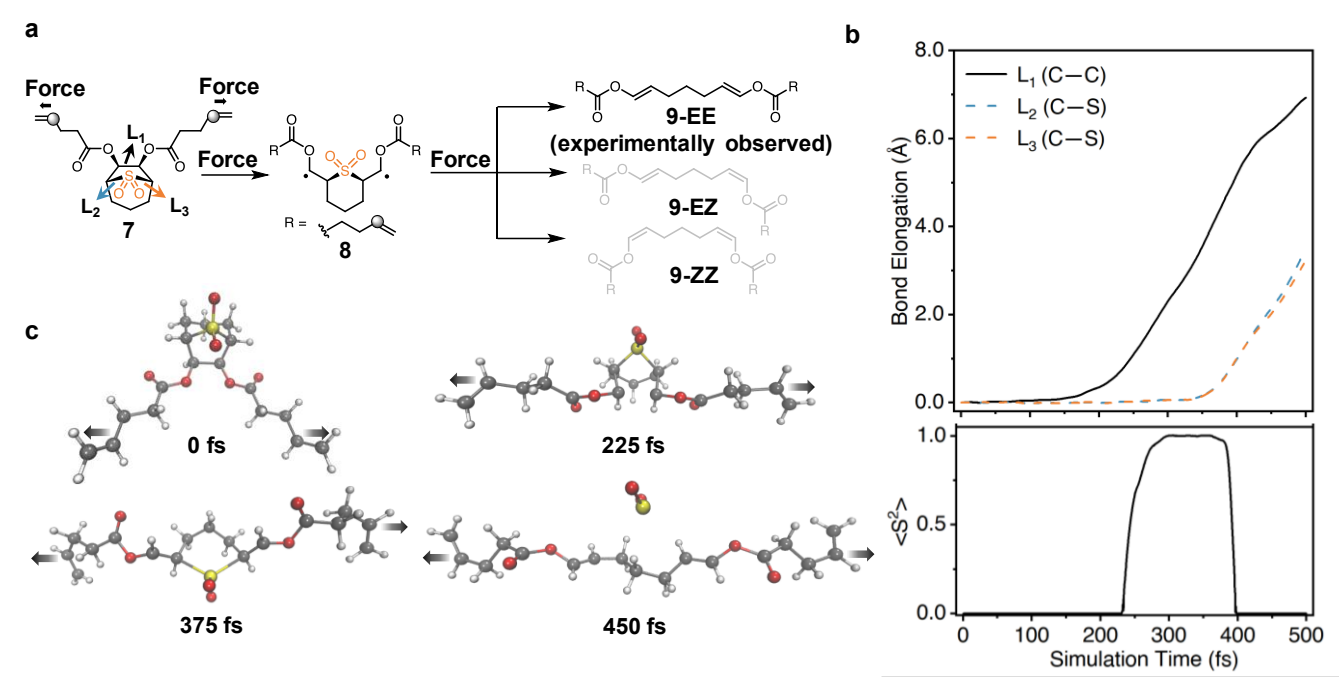


Figure 5. a) Proposed stepwise mechanism of 7 opening and the potentially generated stereoisomers. The grey sphere represents the atom to where the force is applied. b) Top: Profile of key bond elongations of TBO under 2.0 nN of force in AISMD simulations. Bottom: $\langle S^2 \rangle$ values of **TBO** under 2.0 nN of force during the AISMD simulation. c) Snapshots from representative AISMD runs of 7 using an external force of 2.0 nN. Instantaneous external force is depicted as black arrows.

triggered release of both SO_2 and stored length) is appealing, as tougher networks enable greater stress to be loaded into a material and, as a result, higher levels of cargo release to be obtained. We therefore speculate that the dual functions of **TBO** might be synergistic.

The force-coupled rate constants of TBO opening were extracted from both CV and single-event FC experiments (Figure S30). Rate constants were determined in two ways. In the FC experiments, distance vs. time data were fit to a single exponential decay (first order rate law) to obtain a rate constant at the applied clamping force. In the CV SMFS experiments, force-coupled rate constants were obtained by fitting the plateau region to a kinetic model that accounts for and extracts the change in rate as the force varies across the pull. Combining these data gives rate constant k(f) as a function of force. For the data shown in Figure 3a, at the 1520 pN f* typical of the CV SMFS experiments, the rate constant was determined to be 9.0 s⁻¹, whereas the rate constant at 1440 pN in the FC experiments was found to be 1.8 s⁻¹. The full range of extracted rate vs. force data across multiple CV and FC SMFS experiments are provided in Figure S30. According to the simplest model of mechanochemical coupling (eq 1),⁷⁵

$$\ln(k(f)) = C + \frac{F\Delta x^{\ddagger}}{RT}$$
 (1)

the empirical mechanochemical coupling constant Δx^{\ddagger} was calculated to be 0.82 ± 0.2 Å. The number is comparable to the reported values on **NEO** mechanophores. Because Δx^{\ddagger} is strongly associated with the structure of the transition state relative to reactant, the agreement between **TBO** and **NEO** suggests a similar mechanism for the two mechanophores, ⁶⁵ previously attributed to a rate-limiting step of the initial C–C bond cleavage under ~ 1.5 nN force. ⁵⁶

We note that whereas many covalent reactions of mechanophores have been characterized by SMFS, very few reports have demonstrated individually resolved activation events. 70,76,77 Those rare examples have been limited to macrocyclic cyclobutane mechanophores that have a sufficiently large stored length (> 3 nm per event). The resolved single activation event of relatively small **TBO** domains (~ 0.68 nm) in FC implies the possibility of further generalizing the scope of covalent mechanophores in single-event spectroscopy. The FC spectroscopy has been widely used to study protein unfolding 78-80 and the current results suggest that it may hold unique advantages compared to CV pulls for the study of covalent mechanophores.

Mechanistic Study of TBO Mechanophore. We first computationally investigated the activation of TBO using constrained geometries simulate external force (CoGEF) as a widely applied screening tool. We observed SO₂ extrusion with a relatively low rupture force (F_{max}) of 3.3 nN (Figure S37). CoGEF suggests a one-step transformation that involves simultaneous C–C bond scission and SO₂ release using a step increment of 0.1 Å, in contrast to the previous stepwise process observed in the NEO mechanophores. Se Intriguingly, a stepwise mechanism was observed instead when using a smaller step increment of 0.05 Å near bond cleavages (Figure S38). CoGEF is well-known to omit thermal and dynamic effects, We thus reasoned the mechanochemical activation of TBO merits more systematic computational studies with a higher-level method.

We employed *ab initio* steered molecular dynamics (AISMD) to investigate the mechanochemical opening of 7 under different forces from 1.5 to 2.5 nN during 500 fs durations at 300 K using uB3LYP-D3BJ/6-31G* (**Figure 5a**). Only about 10% of the population proceeded to 9 under 1.5 nN within the 500 fs timeframe of dynamic simulation. With the application of 2.0 nN force, we saw successful opening of 7 to 9 in all 30 trajectories. By following the bond elongation over time, we observed the first C–C bond scission event after \sim 225 fs to generate 8 (**Figure 5b and 5c**). The < S² > values (i.e., the

expectation values of S² operator) were also calculated during the simulation to analyze the reaction mechanism (Figure 5b **bottom**). The rapid increase of $\langle S^2 \rangle$ value up to ~ 1.0 suggests a homolytic cleavage of the first C-C bond to generate a singlet diradical intermediate, indicating a stepwise mechanism that is contrary to CoGEF simulations with a step increment of 0.1 Å. A substantial secondary extension is required to trigger the subsequent SO₂ elimination starting from ~375 fs, evidenced by both the rapidly elongated C-S bonds and a sharp decline of <S²> value with the SO₂ extrusion. The two C-S bonds were cleaved simultaneously, indicating a synchronous radical β -elimination process (Figure 5b top). The diradical lifetime was estimated to be ~ 630 fs under 2.0 nN. At higher forces of 2.25 and 2.50 nN, the stepwise nature of 7 opening remains unchanged despite the accelerated kinetics (Figure S40). Decreased diradical lifetime was observed with the increase of applied force (**Table S8**).

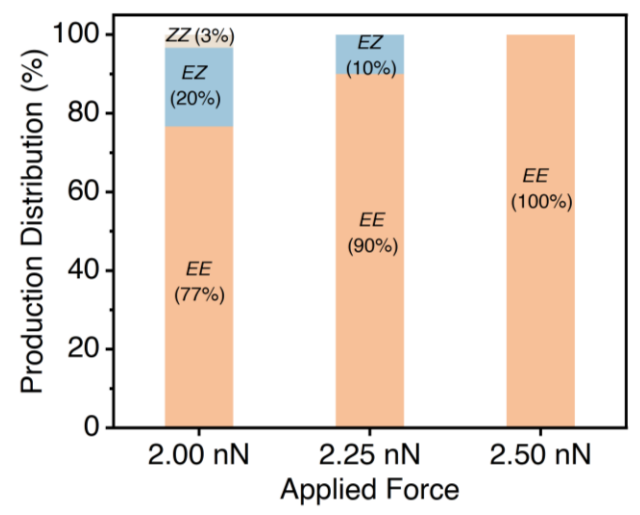


Figure 6. Simulated stereochemical outcomes of 7 opening under different forces in AISMD simulations.

We next analyzed the stereochemical distribution of the formed olefin products **9** from the AISMD results. ⁸² Under relatively low force of 2.0 nN, all three possible isomers were observed with the distribution of 77% EE, 20% EZ, and 3% ZZ (**Figure 6**). With the increase of force, the opening of **7** tends to be more stereoselective towards the EE configuration. A sole EE isomer formation was observed computationally under a high force value of 2.5 nN. Therefore, large forces not only effectively accelerate the **TBO** activation but also drive the reaction into a single product, accounting for the observed facile activation and near quantitative product selectivity in the μ s time scale of sonochemical conditions. ⁸³ This increased stereoselectivity towards the stereoretentive product at high forces was also reported in the flyby trajectories of cyclobutane mechanophore ring-opening. ⁸⁴

The isomeric configuration of mechanophore is known to dramatically impact its mechanochemical reactivity. 56,62,85 We therefore sought to investigate the reactivity of the other two configurations of **TBO** (i.e., *endo* and *trans*) (**Table S9**). Different from the facile opening of all trajectories of 7 under 2.0 nN in AISMD within 500 fs, only about 10% of the population of *endo*-**TBO** were activated under 2.0 nN, indicating the diminished reactivity in the *endo* configuration. The *trans*-**TBO** exhibited an even more limited mechanochemical reactivity that no dissociations were

observed at 3.0 nN of force within 500 fs. Experimentally accessing the *endo-* and *trans-***TBO** will be helpful to further validate the computed reactivity trend, however, the synthesis of these two stereoisomers has been challenging despite the extensive synthetic efforts (**Figure S24**).

CONCLUSION

In summary, we have demonstrated TBO as a new SO2 donor that is thermally stable but can be selectively activated by mechanical force. The non-scissile nature of TBO enables the release of >200 SO₂ molecules per polymer chain in either organic solvent or water upon pulsed ultrasonication. The activation of TBO was quantified and resolved at the singleevent level in SMFS, suggesting a moderate reactivity among C-C bond scission mechanophores with the release of ~ 0.68 nm stored length per unit. Computational studies suggest a stepwise mechanism and provide insights on diradical lifetime and product stereoselectivity. Notably, the development of TBO, in addition to the previous NEO scaffold, 49,56 demonstrates a conceivably general diradical-elimination cascade strategy to release multiple GSMs per chain. This strategy involves two key design principles. First, a bicyclic moiety is required to ensure the non-scissile nature of mechanophores for multiple activation events per chain. Second, after the presumably rate-determining homolytic bond scission, an appropriate leaving group located in the bridge position is needed that readily undergoes β -elimination from the mechanodiradicals. Our work also complements other general cargo releasing mechanophore scaffolds that are promising but may not be readily adaptable for GSMs delivery, 26,48 facilitating the translation of polymer mechanochemistry to potential biomedical applications.

ASSOCIATED CONTENT

The supporting information is available free of charge via the Internet at http://pubs.acs.org.

Detailed descriptions of synthetic procedures, experimental methods, ultrsonication characterizations, SMFS results, and computational details.

CCDC 2322909, 2322911 contain the supplementary crystallographic data for this paper. These data can be obtained free of charge via www.ccdc.cam.ac.uk/data_request/cif, or by emailing data_request@ccdc.cam.ac.uk, or by contacting The Cambridge Crystallographic Data Centre, 12 Union Road, Cambridge CB2 1EZ, UK; fax: +44 1223 336033.

AUTHOR INFORMATION

Corresponding Author

* Heather J. Kulik – Department of Chemical Engineering and Department of Chemistry, Massachusetts Institute of Technology; Cambridge, Massachusetts, 02139, United States; Email: hjkulik@mit.edu

* Stephen L. Craig – Department of Chemistry, Duke University, Durham, North Carolina 27708, United States; Email: stephen.craig@duke.edu

* Jeffery S. Moore – Department of Chemistry and Beckman Institute for Advanced Science and Technology, University of Illinois at Urbana-Champaign, Urbana, Illinois 61801, United States; Email: jsmoore@illinois.edu

Authors

Yunyan Sun – Department of Chemistry and Beckman Institute for Advanced Science and Technology, University of Illinois at Urbana-Champaign, Urbana, Illinois 61801, United States;

Willian J. Neary – Department of Chemistry and Beckman Institute for Advanced Science and Technology, University of Illinois at Urbana-Champaign, Urbana, Illinois 61801, United States; Xiao Huang – Department of Chemistry, Massachusetts Institute of Technology; Cambridge, Massachusetts, 02139, United States; Tatiana B. Kouznetsova – Department of Chemistry, Duke University, Durham, North Carolina 27708, United States;

Tetsu Ouchi – Department of Chemistry, Duke University, Durham, North Carolina 27708, United States;

Ilia Kevlishvili – Department of Chemical Engineering, Massachusetts Institute of Technology; Cambridge, Massachusetts, 02139, United States;

Kecheng Wang – Department of Chemistry, University of Illinois at Urbana-Champaign, Urbana, Illinois 61801, United States; Yingying Chen – Department of Material Science and Engineering and Beckman Institute for Advanced Science and Technology, University of Illinois at Urbana-Champaign, Urbana, Illinois 61801, United States;

Present Addresses

† Department of Chemistry, University of California, Riverside, Riverside, California 92521, United States;

Funding Sources

This work was supported by the NSF Center for the Chemistry of Molecularly Optimized Networks (MONET), CHE-2116298.

Notes

The authors declare no competing financial interest.

ACKNOWLEDGMENT

This work was supported by the NSF Center for the Chemistry of Molecularly Optimized Networks (MONET), CHE-2116298. The authors thank Toby Woods for collecting crystal data, Dorothy Loudermilk for graphic assistance. Thermogravimetric analysis experiments were carried out in the Materials Research Laboratory Central Research Facilities, University of Illinois.

REFERENCES

- (1) Ough, C. S.; Crowell, E. A. Use of Sulfur Dioxide in Winemaking. *J. Food. Sci.* **1987**, *52*, 386–388.
- (2) Belén García-Alonso, M.; Pena-Egido, J.; García-Moreno, C. S-Sulfonate Determination and Formation in Meat Products. *J. Agric. Food. Chem.* **2001**, *49*, 423–429.
- (3) Li, Z. G.; Li, X. E.; Chen, H. Y. Sulfur Dioxide: An Emerging Signaling Molecule in Plants. *Front. Plant. Sci.* **2022**, *13*, 891626.
- (4) Yu, W.; Jin, H.; Tang, C.; Du, J.; Zhang, Z. Sulfur-Containing Gaseous Signal Molecules, Ion Channels and Cardiovascular Diseases. *Br. J. Pharmacol.* **2018**, *175*, 1114–1125.
- (5) Huang, Y.; Tang, C.; Du, J.; Jin, H. Endogenous Sulfur Dioxide: A New Member of Gasotransmitter Family in the Cardiovascular System. *Oxid. Med. Cell. Longev.* **2016**, 8961951.
- (6) Wang, W.; Wang, B. SO₂ Donors and Prodrugs, and Their Possible Applications: A Review. *Front. Chem.* **2018**, *6*, 559.
- (7) Qin, G.; Wu, M.; Wang, J.; Xu, Z.; Xia, J.; Sang, N. Sulfur Dioxide Contributes to the Cardiac and Mitochondrial Dysfunction in Rats. *Toxicol. Sci.* **2016**, *151*, 334–336.
- (8) Langley-Evans, S. C.; Phillips, G. J.; Jackson, A. A. Sulphur Dioxide: A Potent Glutathione Depleting Agent. *Comp. Biochem. Physiol. C Toxicol. Pharmacol* **1996**, *114*, 89–98.
- (9) Kodama, R.; Sumaru, K.; Morishita, K.; Kanamori, T.; Hyodo, K.; Kamitanaka, T.; Morimoto, M.; Yokojima, S.; Nakamura,

- S.; Uchida, K. A Diarylethene as the SO₂ Gas Generator upon UV Irradiation. *Chem. Commun.* **2015**, *51*, 1736–1738.
- (10) Malwal, S. R.; Chakrapani, H. Benzosulfones as Photochemically Activated Sulfur Dioxide (SO₂) Donors. *Org. Biomol. Chem.* **2015**, *13*, 2399–2406.
- (11) Venkatesh, Y.; Kiran, K. S.; Shah, S. S.; Chaudhuri, A.; Dey, S.; Singh, N. D. P. One- and Two-Photon Responsive Sulfur Dioxide (SO₂) Donors: A Combinatorial Drug Delivery for Improved Antibiotic Therapy. *Org. Biomol. Chem.* **2019**, *17*, 2640–2645.
- (12) Malwal, S. R.; Gudem, M.; Hazra, A.; Chakrapani, H. Benzosultines as Sulfur Dioxide (SO₂) Donors. *Org. Lett.* **2013**, *15*, 1116–1119.
- (13) Wang, W.; Ji, X.; Du, Z.; Wang, B. Sulfur Dioxide Prodrugs: Triggered Release of SO₂ via a Click Reaction. *Chem. Commun.* **2017**, *53*, 1370-1373.
- (14) Ji, X.; El-Labbad, E. M.; Ji, K.; Lasheen, D. S.; Serya, R. A. T.; Abouzid, K. A.; Wang, B. Click and Release: SO₂ Prodrugs with Tunable Release Rates. *Org. Lett.* **2017**, *19*, 818–821.
- (15) Day, J. J.; Yang, Z.; Chen, W.; Pacheco, A.; Xian, M. Benzothiazole Sulfinate: A Water-Soluble and Slow-Releasing Sulfur Dioxide Donor. *ACS. Chem. Biol.* **2016**, *11*, 1647–1651.
- (16) Malwal, S. R.; Sriram, D.; Yogeeswari, P.; Konkimalla, V. B.; Chakrapani, H. Design, Synthesis, and Evaluation of Thiol-Activated Sources of Sulfur Dioxide (SO₂) as Antimycobacterial Agents. *J. Med. Chem.* **2012**, *55*, 553–557.
- (17) Wang, W.; Wang, B. Esterase-Sensitive Sulfur Dioxide Prodrugs Inspired by Modified Julia Olefination. *Chem. Commun.* **2017**, *53*, 10124–10127.
- (18) He, P.; Ren, X.; Zhang, Y.; Tang, B.; Xiao, C. Recent Advances in Sulfur Dioxide Releasing Nanoplatforms for Cancer Therapy. *Acta. Biomater.* **2023**, *174*, 91–103.
- (19) El-Labbad, E. M.; Ji, X.; Abouzid, K. A. M.; Wang, B. Medicinal Chemistry Strategies Towards SO₂ Donors as Research Tools and Potential Therapeutics. *Curr. Top. Med. Chem.* **2021**, *21*, 2870–2881.
- (20) Versaw, B. A.; Zeng, T.; Hu, X.; Robb, M. J. Harnessing the Power of Force: Development of Mechanophores for Molecular Release. *J. Am. Chem. Soc.* **2021**, *143*, 21461–21473.
- (21) Shen, H.; Cao, Y.; Lv, M.; Sheng, Q.; Zhang, Z. Polymer Mechanochemistry for the Release of Small Cargoes. *Chem. Commun.* **2022**, *58*, 4813-4824.
- (22) Küng, R.; Göstl, R.; Schmidt, B. M. Release of Molecular Cargo from Polymer Systems by Mechanochemistry. *Chem. Eur. J.* **2022**, *28*, e202103860.
- (23) Li, J.; Nagamani, C.; Moore, J. S. Polymer Mechanochemistry: From Destructive to Productive. *Acc. Chem. Res.* **2015**, *48*, 2181–2190.
- (24) Caruso, M. M.; Davis, D. A.; Shen, Q.; Odom, S. A.; Sottos, N. R.; White, S. R.; Moore, J. S. Mechanically-Induced Chemical Changes in Polymeric Materials. *Chem. Rev.* **2009**, *109*, 5755–5798.
- (25) Davis, D. A.; Hamilton, A.; Yang, J.; Cremar, L. D.; Van Gough, D.; Potisek, S. L.; Ong, M. T.; Braun, P. V.; Martínez, T. J.; White, S. R.; Moore, J. S.; Sottos, N. R. Force-Induced Activation of Covalent Bonds in Mechanoresponsive Polymeric Materials. *Nature* **2009**, *459*, 68–72.
- (26) Huo, S.; Zhao, P.; Shi, Z.; Zou, M.; Yang, X.; Warszawik, E.; Loznik, M.; Göstl, R.; Herrmann, A. Mechanochemical Bond Scission for the Activation of Drugs. *Nat. Chem.* **2021**, *13*, 131–139.
- (27) May, P. A.; Moore, J. S. Polymer Mechanochemistry: Techniques to Generate Molecular Force via Elongational Flows. *Chem. Soc. Rev.* **2013**, *42*, 7497-7506.
- (28) Zhao, P.; Huo, S.; Fan, J.; Chen, J.; Kiessling, F.; Boersma, A. J.; Göstl, R.; Herrmann, A. Activation of the Catalytic Activity of Thrombin for Fibrin Formation by Ultrasound. *Angew. Chem.* **2021**, *60*, 14707-14714.
- (29) Yao, Y.; McFadden, M. E.; Luo, S. M.; Barber, R. W.; Kang, E.; Bar-Zion, A.; Smith, C. A. B.; Jin, Z.; Legendre, M.; Ling, B.; Malounda, D.; Torres, A.; Hamza, T.; Edwards, C. E. R.; Shapiro, M. G.; Robb, M. J. Remote Control of Mechanochemical Reactions under Physiological Conditions Using Biocompatible Focused Ultrasound. *Proc. Natl. Acad. Sci. U. S. A.* 2023, 120, e2309822120.

- (30) Kim, G.; Lau, V. M.; Halmes, A. J.; Oelze, M. L.; Moore, J. S.; Li, K. C. High-Intensity Focused Ultrasound-Induced Mechanochemical Transduction in Synthetic Elastomers. *Proc. Natl. Acad. Sci. U. S. A.* **2019**, *116*, 10214–10222.
- (31) Kim, G.; Wu, Q.; Chu, J. L.; Smith, E. J.; Oelze, M. L.; Moore, J. S.; Li, K. C. Ultrasound Controlled Mechanophore Activation in Hydrogels for Cancer Therapy. *Proc. Natl. Acad. Sci. U. S. A.* **2022**, *119* (4), e2109791119.
- (32) Küng, R.; Pausch, T.; Rasch, D.; Göstl, R.; Schmidt, B. M. Mechanochemical Release of Non-Covalently Bound Guests from a Polymer-Decorated Supramolecular Cage. *Angew. Chem.* **2021**, *60*, 13626–13630.
- (33) Larsen, M. B.; Boydston, A. J. "Flex-Activated" Mechanophores: Using Polymer Mechanochemistry to Direct Bond Bending Activation. *J. Am. Chem. Soc.* **2013**, *135*, 8189–8192.
- (34) Shen, H.; Larsen, M. B.; Roessler, A. G.; Zimmerman, P. M.; Boydston, A. J. Mechanochemical Release of N-Heterocyclic Carbenes from Flex-Activated Mechanophores. *Angew. Chem. Int. Ed.* **2021**, *60*, 13559–13563.
- (35) Hu, X.; Zeng, T.; Husic, C. C.; Robb, M. J. Mechanically Triggered Small Molecule Release from a Masked Furfuryl Carbonate. *J. Am. Chem. Soc.* **2019**, *141*, 15018–15023.
- (36) Yang, F.; Geng, T.; Shen, H.; Kou, Y.; Xiao, G.; Zou, B.; Chen, Y. Mechanochemical Release of Fluorophores from a "Flex-Activated" Mechanophore. *Angew. Chem. Int. Ed.* **2023**, *62*, e202308662.
- (37) Shi, Z.; Wu, J.; Song, Q.; Göstl, R.; Herrmann, A. Toward Drug Release Using Polymer Mechanochemical Disulfide Scission. *J. Am. Chem. Soc.* **2020**, *142*, 14725–14732.
- (38) He, X.; Tian, Y.; O'Neill, R. T.; Xu, Y.; Lin, Y.; Weng, W.; Boulatov, R. Coumarin Dimer Is an Effective Photomechanochemical AND Gate for Small-Molecule Release. *J. Am. Chem. Soc.* **2023**, *145*, 23214–23226.
- (39) Lu, Y.; Sugita, H.; Mikami, K.; Aoki, D.; Otsuka, H. Mechanochemical Reactions of Bis(9-Methylphenyl-9-Fluorenyl) Peroxides and Their Applications in Cross-Linked Polymers. *J. Am. Chem. Soc.* **2021**, *143*, 17744–17750.
- (40) Yang, J.; Xia, Y. Force-Triggered Guest Release from Mechanophore Incorporated Rotaxanes. *CCS. Chem.* **2023**, *5*, 1365-1371.
- (41) Suwada, K.; Ieong, A. W.; Lo, H. L. H.; De Bo, G. Furan Release via Force-Promoted Retro-[4+2][3+2] Cycloaddition. *J. Am. Chem. Soc.* **2023**, *145*, 20782–20785.
- (42) Diesendruck, C. E.; Steinberg, B. D.; Sugai, N.; Silberstein, M. N.; Sottos, N. R.; White, S. R.; Braun, P. V.; Moore, J. S. Proton-Coupled Mechanochemical Transduction: A Mechanogenerated Acid. *J. Am. Chem. Soc.* **2012**, *134*,12446–12449.
- (43) Lin, Y.; Kouznetsova, T. B.; Craig, S. L. A Latent Mechanoacid for Time-Stamped Mechanochromism and Chemical Signaling in Polymeric Materials. *J. Am. Chem. Soc.* **2020**, *142*, 99–103.
- (44) Hu, X.; Zeng, T.; Husic, C. C.; Robb, M. J. Mechanically Triggered Release of Functionally Diverse Molecular Payloads from Masked 2-Furylcarbinol Derivatives. *ACS. Cent. Sci.* **2021**, *7*, 1216–1224.
- (45) Huo, S.; Liao, Z.; Zhao, P.; Zhou, Y.; Göstl, R.; Herrmann, A. Mechano-Nanoswitches for Ultrasound-Controlled Drug Activation. *Adv. Sci.* **2022**, *9*, 2104696.
- (46) Di Giannantonio, M.; Ayer, M. A.; Verde-Sesto, E.; Lattuada, M.; Weder, C.; Fromm, K. M. Triggered Metal Ion Release and Oxidation: Ferrocene as a Mechanophore in Polymers. *Angew. Chem. Int. Ed.* **2018**, *57*,11445–11450.
- (47) Nijem, S.; Song, Y.; Schwarz, R.; Diesendruck, C. E. Flex-Activated CO Mechanochemical Production for Mechanical Damage Detection. *Polym. Chem.* **2022**, *13*, 3986–3990.
- (48) Zeng, T.; Ordner, L. A.; Liu, P.; Robb, M. J. Multi-Mechanophore Polymers for Mechanically Triggered Small Molecule Release with Ultrahigh Payload Capacity. *J. Am. Chem. Soc.* **2024**, *146*, 95–100.
- (49) Sun, Y.; Neary, W. J.; Burke, Z. P.; Qian, H.; Zhu, L.; Moore, J. S. Mechanically Triggered Carbon Monoxide Release with

- Turn-On Aggregation-Induced Emission. J. Am. Chem. Soc. 2022, 144,1125-1129.
- (50) Raasch, M. S. Annelations with Tetrachlorothiophene 1,1-Dioxide. *J. Org. Chem.* **1980**, *45*, 856–867.
- (51) Birch, S. F.; Dean, R. A.; Hunter, N. J.; Whitehead, E. V. Preparation and Physical Properties of Sulfur Compounds Related to Petroleum. VII. 2-, 6- and 8-Thiabicyclo[3.2.1]Octane and 2-Thiabicyclo[2.2.2]Octane. *J. Org. Chem.* **1957**, *22*, 1590–1594.
- (52) Dupau, P.; Epple, R.; Thomas, A. A.; Fokin, V. V.; Sharpless, K. B. Osmium-Catalyzed Dihydroxylation of Olefins in Acidic Media: Old Process, New Tricks. *Adv. Synth. Catal.* **2002**, *344*, 421–433
- (53) Grayson, S. M.; Long, B. K.; Kusomoto, S.; Osborn, B. P.; Callahan, R. P.; Chambers, C. R.; Willson, C. G. Synthesis and Characterization of Norbornanediol Isomers and Their Fluorinated Analogues. *J. Org. Chem.* **2006**, *71*, 341–344.
- (54) Bowser, B. H.; Craig, S. L. Empowering Mechanochemistry with Multi-Mechanophore Polymer Architectures. *Polym. Chem.*, **2018**, *9*, 3583-3593.
- (55) Wu, D.; Lenhardt, J. M.; Black, A. L.; Akhremitchev, B. B.; Craig, S. L. Molecular Stress Relief through a Force-Induced Irreversible Extension in Polymer Contour Length. *J. Am. Chem. Soc.* **2010**, *132*, 15936–15938.
- (56) Sun, Y.; Kevlishvili, I.; Kouznetsova, T. B.; Burke, Z. P.; Craig, S. L.; Kulik, H. J.; Moore, J. S. The Tension Activated Carbon–Carbon Bond. *ChemRxiv* **2023**. DOI: 10.26434/chemrxiv-2023-rzwhn. (accessed 2024-03-27)
- (57) Sun, Y. Q.; Liu, J.; Zhang, J.; Yang, T.; Guo, W. Fluorescent Probe for Biological Gas SO2 Derivatives Bisulfite and Sulfite. *Chem. Commun.*, **2013**, *49*, 2637–2639.
- (58) Infrared Spectroscopy Absorption Table. https://chem.libretexts.org/Ancillary_Materials/Reference/Reference_Tables/Spectroscopy_Absorption_Table. (accessed 2024-02-02)
- (59) Kumar, K.; Goodwin, A. P. Alternating Sulfone Copolymers Depolymerize in Response to Both Chemical and Mechanical Stimuli. *ACS. Macro. Lett.*, **2015**, *4*, 907–911.
- (60) Wang, X. B.; Du, J. B.; Cui, H. Sulfur Dioxide, a Double-Faced Molecule in Mammals. *Life Sci.* **2014**, *98*, 63–67.
- (61) Hsu, T. G.; Zhou, J.; Su, H. W.; Schrage, B. R.; Ziegler, C. J.; Wang, J. A Polymer with "Locked" Degradability: Superior Backbone Stability and Accessible Degradability Enabled by Mechanophore Installation. J. Am. Chem. Soc. 2020, 142, 2100–2104.
- (62) Li, Y.; Xue, B.; Yang, J.; Jiang, J.; Liu, J.; Zhou, Y.; Zhang, J.; Wu, M.; Yuan, Y.; Zhu, Z.; Wang, Z. J.; Chen, Y.; Harabuchi, Y.; Nakajima, T.; Wang, W.; Maeda, S.; Gong, J. P.; Cao, Y. Azobenzene as a Photoswitchable Mechanophore. *Nat. Chem.* **2024**, *16*, 446–455.
- (63) Horst, M.; Yang, J.; Meisner, J.; Kouznetsova, T. B.; Martínez, T. J.; Craig, S. L.; Xia, Y. Understanding the Mechanochemistry of Ladder-Type Cyclobutane Mechanophores by Single Molecule Force Spectroscopy. *J. Am. Chem. Soc.* **2021**, *143*, 12328–12334.
- (64) Klukovich, H. M.; Kouznetsova, T. B.; Kean, Z. S.; Lenhardt, J. M.; Craig, S. L. A Backbone Lever-Arm Effect Enhances Polymer Mechanochemistry. *Nat. Chem.* **2013**, *5*, 110–114.
- (65) Wang, J.; Kouznetsova, T. B.; Niu, Z.; Ong, M. T.; Klukovich, H. M.; Rheingold, A. L.; Martinez, T. J.; Craig, S. L. Inducing and Quantifying Forbidden Reactivity with Single-Molecule Polymer Mechanochemistry. *Nat. Chem.* **2015**, *7*, 323–327.
- (66) Gossweiler, G. R.; Kouznetsova, T. B.; Craig, S. L. Force-Rate Characterization of Two Spiropyran-Based Molecular Force Probes. *J. Am. Chem. Soc.* **2015**, *137*, 6148–615.
- (67) Wu, M.; Li, Y.; Yuan, W.; De Bo, G.; Cao, Y.; Chen, Y. Cooperative and Geometry-Dependent Mechanochromic Reactivity through Aromatic Fusion of Two Rhodamines in Polymers. *J. Am. Chem. Soc.* **2022**, *144*, 17120–17128.
- (68) Zhang, H.; Li, X.; Lin, Y.; Gao, F.; Tang, Z.; Su, P.; Zhang, W.; Xu, Y.; Weng, W.; Boulatov, R. Multi-Modal Mechanophores Based on Cinnamate Dimers. *Nat. Commun.* **2017**, *8*, 1147.
- (69) Lin, Y.; Kouznetsova, T. B.; Craig, S. L. Mechanically Gated Degradable Polymers. *J. Am. Chem. Soc.* **2020**, *142*, 2105–2109.

- (70) Bowser, B. H.; Wang, S.; Kouznetsova, T. B.; Beech, H. K.; Olsen, B. D.; Rubinstein, M.; Craig, S. L. Single-Event Spectroscopy and Unravelling Kinetics of Covalent Domains Based on Cyclobutane Mechanophores. *J. Am. Chem. Soc.* **2021**, *143*, 5269–5276.
- (71) Ong, M. T.; Leiding, J.; Tao, H.; Virshup, A. M.; Martínez, T. J. First Principles Dynamics and Minimum Energy Pathways for Mechanochemical Ring Opening of Cyclobutene. *J. Am. Chem. Soc.* **2009**, *131*, 6377–6379.
- (72) Ribas-Arino, J.; Shiga, M.; Marx, D. Understanding Covalent Mechanochemistry. *Angew. Chem. Int. Ed.* **2009**, *48*, 4190–4193.
- (73) Wang, Z.; Zheng, X.; Ouchi, T.; Kouznetsova, T. B.; Beech, H. K.; Av-Ron, S.; Matsuda, T.; Bowser, B. H.; Wang, S.; Johnson, J. A.; Kalow, J. A.; Olsen, B. D.; Gong, J. P.; Rubinstein, M.; Craig, S. L. Toughening Hydrogels through Force-Triggered Chemical Reactions That Lengthen Polymer Strands. *Science* **2021**, *374*, 193–196.
- (74) Ouchi, T.; Bowser, B. H.; Kouznetsova, T. B.; Zheng, X.; Craig, S. L. Strain-Triggered Acidification in a Double-Network Hydrogel Enabled by Multi-Functional Transduction of Molecular Mechanochemistry. *Mater. Horiz.* **2022**, *10*, 585–593.
- (75) Bell, G. I. Models for the Specific Adhesion of Cells to Cells. *Science*. **1978**, *200*, 618–627.
- (76) Tian, Y.; Cao, X.; Li, X.; Zhang, H.; Sun, C. L.; Xu, Y.; Weng, W.; Zhang, W.; Boulatov, R. A Polymer with Mechanochemically Active Hidden Length. *J. Am. Chem. Soc.* **2020**, *142*, 18687–18697.
- (77) Pill, M. F.; Holz, K.; Preußke, N.; Berger, F.; Clausen-Schaumann, H.; Lüning, U.; Beyer, M. K. Mechanochemical Cycloreversion of Cyclobutane Observed at the Single Molecule Level. *Chem. Eur. J.* **2016**, *22*, 12034–12039.

- (78) Hoffmann, T.; Dougan, L. Single Molecule Force Spectroscopy Using Polyproteins. *Chem. Soc. Rev.* **2012**, *41*, 4781–4796.
- (79) Schlierf, M.; Li, H.; Fernandez, J. M. The Unfolding Kinetics of Ubiquitin Captured with Single-Molecule Force-Clamp Techniques. *Proc. Natl. Acad. Sci. U, S, A,* **2004**, *101*, 7299.
- (80) Rivas-Pardo, J. A.; Eckels, E. C.; Popa, I.; Kosuri, P.; Linke, W. A.; Fernández, J. M. Work Done by Titin Protein Folding Assists Muscle Contraction. *Cell, Rep.* **2016**, *14*, 1339–1347.
- (81) Klein, I. M.; Husic, C. C.; Kovács, D. P.; Choquette, N. J.; Robb, M. J. Validation of the CoGEF Method as a Predictive Tool for Polymer Mechanochemistry. *J. Am. Chem. Soc.* **2020**, *142*, 16364–16381.
- (82) Chen, Z.; Zhu, X.; Yang, J.; Mercer, J. A. M.; Burns, N. Z.; Martinez, T. J.; Xia, Y. The Cascade Unzipping of Ladderane Reveals Dynamic Effects in Mechanochemistry. *Nat. Chem.* **2020**, *12*, 302–309.
- (83) Lenhardt, J. M.; Black Ramirez, A. L.; Lee, B.; Kouznetsova, T. B.; Craig, S. L. Mechanistic Insights into the Sonochemical Activation of Multimechanophore Cyclopropanated Polybutadiene Polymers. *Macromolecules* **2015**, *48*, 6396–6403.
- (84) Liu, Y.; Holm, S.; Meisner, J.; Jia, Y.; Wu, Q.; Woods, T. J.; Martinez, T. J.; Moore, J. S. Flyby Reaction Trajectories: Chemical Dynamics under Extrinsic Force. *Science* **2021**, *373*, 208–212.
- (85) Stevenson, R.; De Bo, G. Controlling Reactivity by Geometry in Retro-Diels-Alder Reactions under Tension. *J. Am. Chem. Soc.* **2017**, *139*, 16768–16771.

